ACS Macro Letters

Letter

pubs.acs.org/macroletters

Protonation-Induced Microphase Separation in Thin Films of a Polyelectrolyte-Hydrophilic Diblock Copolymer

Charlotte R. Stewart-Sloan[†] and Bradley D. Olsen*[,‡]

Departments of [†]Materials Science and Engineering and [‡]Chemical Engineering, Massachusetts Institute of Technology, Cambridge, Massachusetts 02139, United States

Supporting Information

ABSTRACT: Block copolymers composed of poly(oligo ethylene glycol methyl ether methacrylate) and poly(2-vinylpyridine) are disordered in the neat state but can be induced to order by protonation of the P2VP block, demonstrating a tunable and responsive method for triggering assembly in thin films. Comparison of protonation with the addition of salts shows that microphase separation is due to selective protonation of the P2VP block. Increasing acid incorporation and increasing 2-vinylpyridine content for P2VP minority copolymers both promote increasingly phase-separated morphologies, consistent with protonation increasing the effective strength of segregation between the two blocks. The self-assembled nanostructures formed after casting from acidic solutions may be tuned based on the amount and type of acid incorporation as well as the annealing treatment applied after casting, where both aqueous and polar organic solvents are shown to be effective. Therefore, POEGMA-*b*-P2VP is a novel ion-containing block copolymer whose morphologies can be facilely tuned during casting and processing by controlling its exposure to acid.

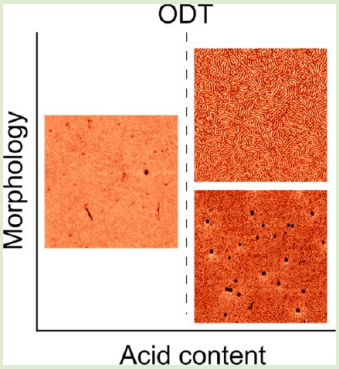

Polyelectrolytes, ionomers, and ion-containing polymers have attracted technological interest due to their ability to control the transport of ions and their improved mechanical properties in comparison to chemically similar ion-free polymers. High ion transport is particularly useful in electrolyte membranes for fuel cells[1] and batteries.[2] For example, the commercial ion-containing polymer Nafion[3] is a particularly effective membrane material since it allows ion but not electron transport. In the case of Li-ion batteries, poly(ethylene glycol) (PEG) has been studied due to its strong ability to coordinate and transport lithium cations.[4] Recent research in this area has also focused on block copolymers because they can be designed to combine one noninteracting block which supplies mechanical stability and one solubilizing block which provides conductive pathways.[5] In many cases, the morphologies of these composite materials have had profound effects on their ion transport properties,[6] making morphology control of central importance. For ion-containing polymers in non-aqueous environments, ion incorporation can be used to improve the mechanical properties of plastics by forming ionic cross-links resulting from the phase separation of ion-rich and ion-poor domains within a material. These polymers typically have two relaxations, with the ion-rich domain glass transition significantly elevated compared to the ion-poor domain transition.[7] As a result, they have been used in applications such as thermoplastic elastomers[8] and shape-memory materials.[9] This technology has been commercialized in the form of Surlyn,[10] used in packaging and coating applications.

Commercially relevant polymers with charged groups covalently attached to the main chain can occupy two extremes of ion content with differing properties: polyelectrolytes where greater than 80% of the monomers are charged and ionomers where less than 10% are charged.[11] Polyelectrolytes are controlled by their uniformity and hydrophilicy, while those of ionomers are determined by the segregation of the highly charged regions from the nonpolar matrix; polymers with intermediate ion content can be water sensitive but not highly soluble.[11] Ionomers can be synthesized by copolymerizing ionic and nonionic monomers[11] or by postfunctionalizing hydrophobic polymers.[11] Block copolymers containing ionomer blocks can be synthesized which have the typical ion-induced microphase separation inside the already phase separated domains.[12] For a given block copolymer with one ionomer block, increasing the fraction of ionized monomers can also induce order−disorder and order−order transitions in the solid state.[13] In the liquid state, the number of ionized groups on a polymer chain can also affect the resultant morphologies: P2VP homopolymers transition from a hydrophobic coil surrounded by charged groups into an extended coil[14] as the level of charging increases and pH can be used to tune the size of diblock copolymer micelles formed from weak polyelectrolytes.[15]

Salt doping provides an alternative method to introduce ions into polymers for polar polymers such as PEG, poly(2-vinylpyridine) (P2VP), and poly(methyl methacrylate) (PMMA). When one of these is paired with an ion-rejecting polymer in a block copolymer, the ions will selectively partition and increase the strength of segregation between blocks[16] due to the favorability of ion solvation in the medium with a higher

Received: December 25, 2013
Accepted: March 20, 2014
Published: April 11, 2014

dx.doi.org/10.1021/mz400650q | *ACS Macro Lett.* 2014, 3, 410−414

dielectric constant that outweighs the reduction in entropy of both the polymer chains and the salt ions due to demixing.[17] This yields an increase in the domain spacing and the long-range order.[16e,18]

This letter reports a new double hydrophilic block copolymer (Scheme 1) whose microphase separation can be tuned

Scheme 1. Synthesis of POEGMA-P2VP Block Copolymer

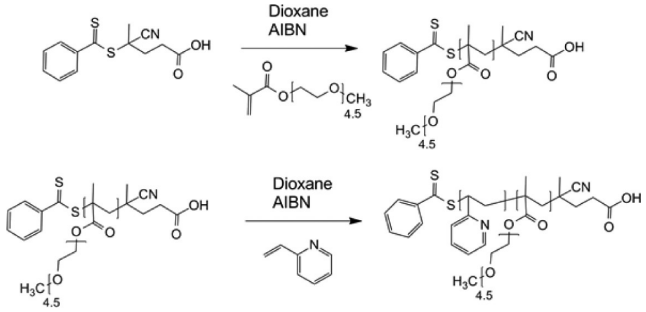

responsively by the protonation/deprotonation of its acid-responsive block. The self-assembly of nonionic-cationic poly(oligoethylene glycol methyl ether methacrylate)-poly(2-vinylpyridine) (POEGMA-P2VP) as a function of acid content is characterized in thin films. This polymer has a segregation strength that is controlled by the degree of protonation of the P2VP block, meaning that the order−disorder transition can be easily tuned by the composition of the casting solution. It is shown that charging, not ion solvation, leads to microphase separation in a manner analogous to the charging of ionomers. Acidic, basic, and neutral aqueous-based solvent vapor annealing techniques are also exploited and compared to traditional organic solvent vapor treatments, demonstrating processing under both traditional and aqueous conditions.

For this work, two model POEGMA-P2VP block copolymers with P2VP minority blocks were synthesized and self-assembled in thin films. Their molecular weights, polydispersities, and block ratios are displayed in Table 1. The added acid nearly

Table 1. Molar Mass Data for POEGMA-P2VP Block Copolymers[a]

name	M_n (PDI) POEGMA	M_n P2VP (Copolymer PDI)	volume fraction P2VP[b]
POEGMA50-P2VP30	50.1 kg/mol (1.19)	29.5 kg/mol (1.24)	0.39
POEGMA43-P2VP13	42.6 kg/mol (1.20)	13.0 kg/mol (1.16)	0.25

[a]Molar masses of POEGMA blocks and PDIs were determined by GPC. The molecular weight of the P2VP blocks were determined by ^{1}H NMR. [b]Volume fractions were calculated by using the densities of 1.25 g/cm^3 for POEGMA[23] and 1.14 g/cm^3 for P2VP.[24]

stoichiometrically protonates 2VP groups due to the large differences in the pK_a values of the different conjugate acid species (4.5 for P2VP,[19] −1.7 for water, −2.4 for ethanol,[20] and −3.5 for POEGMA[21]). In microphase-separated systems, the counterion must be localized within the protonated P2VP nanodomains to preserve charge neutrality, while in disordered films the counterions may be distributed throughout the material. The substrate interface was rendered POEGMA-preferential by PEG brushes grafted to the Si substrate, while the free surface shows little preference for either block due to the minor difference in surface energy between the components.[22]

Figure 1 shows the self-assembled films at varying hydrochloric acid content after annealing in DMSO vapor for 24 h (see Figure S3 for annealing time dependence). As the amount of acid in the films is increased, the films first become inhomogeneous and then display microphase-separated morphologies. The acid concentration at which ordered structures are first observed is much larger for POEGMA43-P2VP13 due to its lower molecular weight and more asymmetric composition. The identities of the ordered phases are also different: POEGMA50-P2VP30 displays in-plane cylinders, while POEGMA43-P2VP13 displays hexagonally packed spheres. These morphologies are assigned based on the two-dimensional projections of the morphologies (two-dimensional stripes and dots, respectively), wetting conditions that favor POEGMA wetting at the substrate and nonpreferential wetting at the free surface, and minority P2VP volume fractions (39% in the case of POEGMA50-P2VP30 and 25% for POEGMA43-P2VP13).

Comparison of thin film nanostructures with a given acid loading to those with equal molar amounts of salt indicates that the block copolymers microphase separate due to ionic interactions similar to those present in ionomers, not due to salt solvation. Figure 2 shows films of POEGMA50-P2VP30 doped with HCl, HI, NaCl, and NaI. These films were doped at a stoichiometry of 0.55 relative to the pyridyl monomer and were annealed in DMSO. In the case of NaI, irregular structures with dimensions bigger than the copolymer molecular dimension are observed; these are hypothesized to result from salt that cannot be solubilized by the polymer. While the acid-containing films are microphase separated, the salt-containing films are not. According to Wang's theory of salt solubilization in polymers,[25] differences in dielectric constant between polymers can lead to differential solibilization that may drive phase separation. However, the failure of salt to induce microphase separation indicates that this effect is not responsible for structure formation. Because of the strong pK_a preference for the formation of the pyridinium chloride or iodide salts, the introduction of acid turns P2VP into an ionomer with varying degrees of neutralization. Counterions must remain close to the highly charged P2VP block in order to maintain charge neutrality. The resultant microphase separation is therefore hypothesized to be due to incompatibility between the protonated and unprotonated blocks in a manner similar to that observed in ionomers.

The rapid removal of solvent after completion of annealing in DMSO leads to vitrification of the P2VP blocks, resulting in morphologies that are kinetically trapped, reflecting structures formed in the solvent-swollen films. However, DMSO is a good solvent for P2VP, POEGMA, and protonated P2VP, indicating that the dilution approximation[26] applies to this block copolymers system. Because this approximation says that the presence of solvent should promote miscibility between blocks, the transition from disordered to microphase separated structures with increasing protonation is due to increased repulsive interactions between the blocks.

In order to better understand the generality of protonation-induced phase separation in neat copolymers, films charged with different counterions and annealed in the vapors of different solvents were compared. Because protonated POEGMA-P2VP is soluble in both polar organic and aqueous solvents, these films can be annealed in solvents capable of a

dx.doi.org/10.1021/mz400650q | ACS Macro Lett. 2014, 3, 410−414

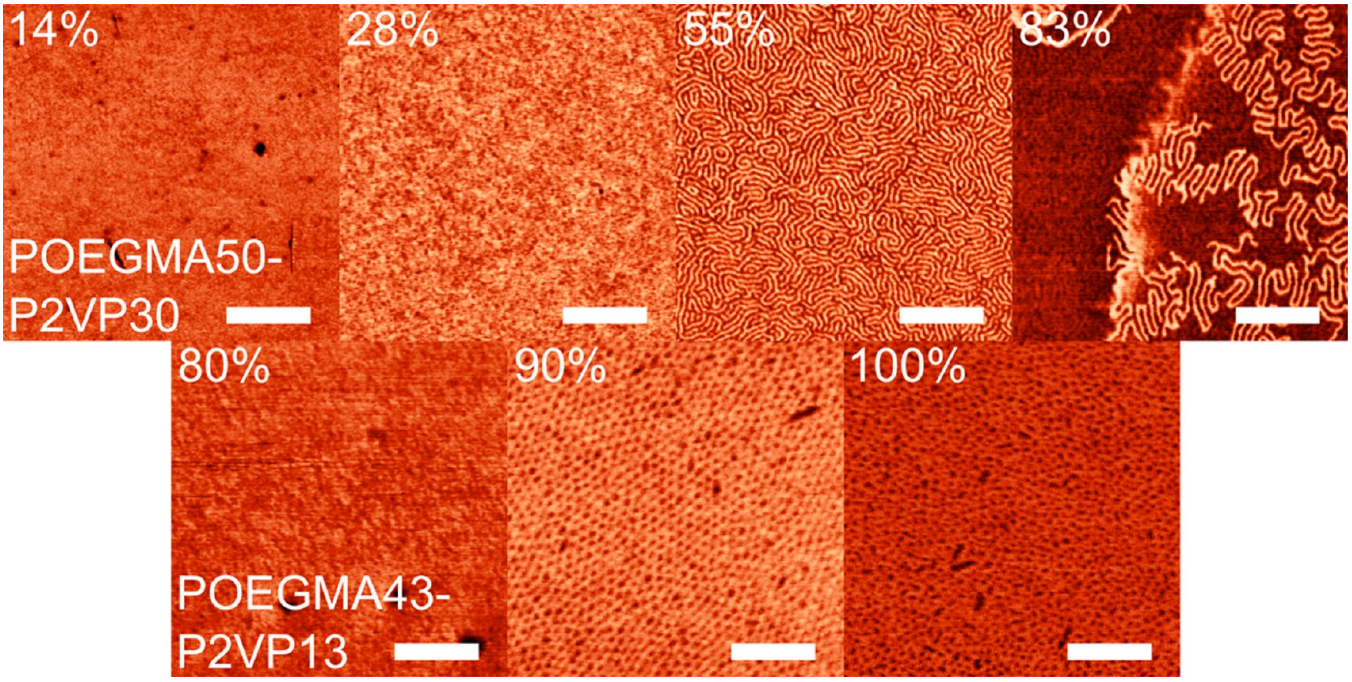

Figure 1. Microphase separation of neat block copolymer films with increasing acid content. Phase images of POEGMA50-P2VP30 (top row) and POEGMA43-P2VP13 (bottom row) films cast with differing stoichiometric amounts of acid per P2VP group (indicated in top left corner of each micrograph) and then annealed in DMSO for one day. POEGMA43-P2VP13 films with less than 80% HCl dewet upon annealing in DMSO. The scale bars for the POEGMA50-P2VP30 films are 50 nm and the phase *z*-range is 25°; the scale bars for the POEGMA43-P2VP13 films are 250 nm and the phase *z*-range is 25°.

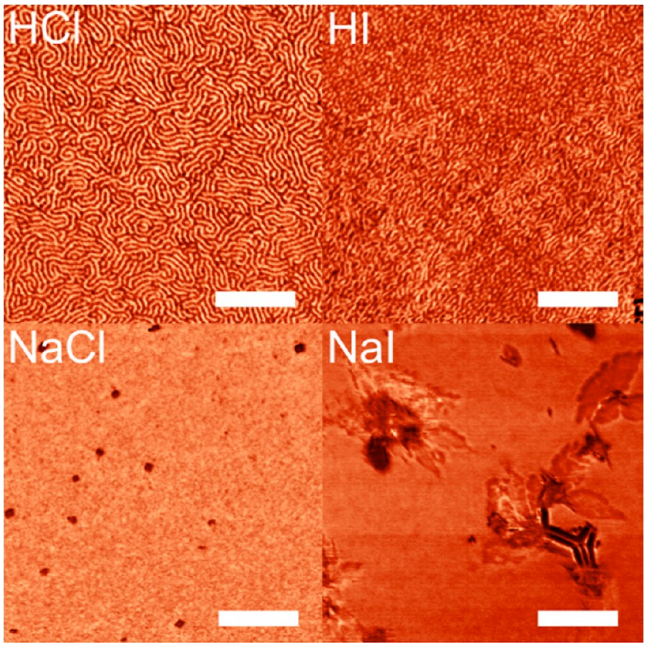

Figure 2. Phase images comparing the effects of NaCl, NaI, HCl, and HI on the morphologies of POEGMA50-P2VP30 thin films at 55% ion loading relative to 2VP monomer. All scale bars are 50 nm and the phase *z*-range is 25°.

variety of possible interactions with both the protonated P2VP and the counterion. Figure 3 shows the results of this experiment for POEGMA50-P2VP30 films at 55% protonation, close to the level of protonation required to trigger the ODT. Initially uncharged films do not display ordered morphologies after any of the annealing treatments shown (images in Figure S10). Two counterions were employed to see if the best annealing treatment depended on the identity of the conjugate base: Cl^- or I^-. Cl^-, which is a harder anion than I^-, should be more closely paired with pyridinium cation and less soluble in organic solvents. In Figure 3, it is apparent that the harder Cl^- anion produces films with better order in the as-cast state than the I^- containing films. After organic solvent annealing, films protonated with HCl always show somewhat better ordering than those cast from HI, particularly in the case of annealing with DMSO. This suggests that the hard Cl^- counterion increases the selectivity of DMSO and DMF, making the solvents more effective at inducing order during solvent annealing. Figure S8 shows the time-dependent morphology evolution for POEGMA43-P2VP13 films cast from 120% stoichiometric HCl and annealed in DMSO, indicating the appropriateness of the 24 h time frame for morphology development during solvent vapor annealing. The disorganized in-plane cylinders present upon casting first coarsen and then transform into smaller close packed spheres over the course of 24 h which are stable until the end of the 48 h experiment, illustrating the strong effect of DMSO vapor on the morphologies of this material.

Solvent annealing in acidic, basic, or ultrapure water vapor is an environmentally friendly processing method for self-assembling polymer films as well as a novel strategy for tuning order. It allows strong solubilization of ions during annealing, as well as dipole−dipole and hydrogen bonding interactions between the solvent and the polymer. Figure 3 shows the effect that these treatments have on both the Cl^- and I^- containing films. In both cases, annealing in the acid vapors provides enhanced segregation and organization, indicating that the presence of acid allows for mobility of both blocks while maintaining or slightly enhancing the protonation of P2VP.

dx.doi.org/10.1021/mz400650q | *ACS Macro Lett.* 2014, 3, 410−414

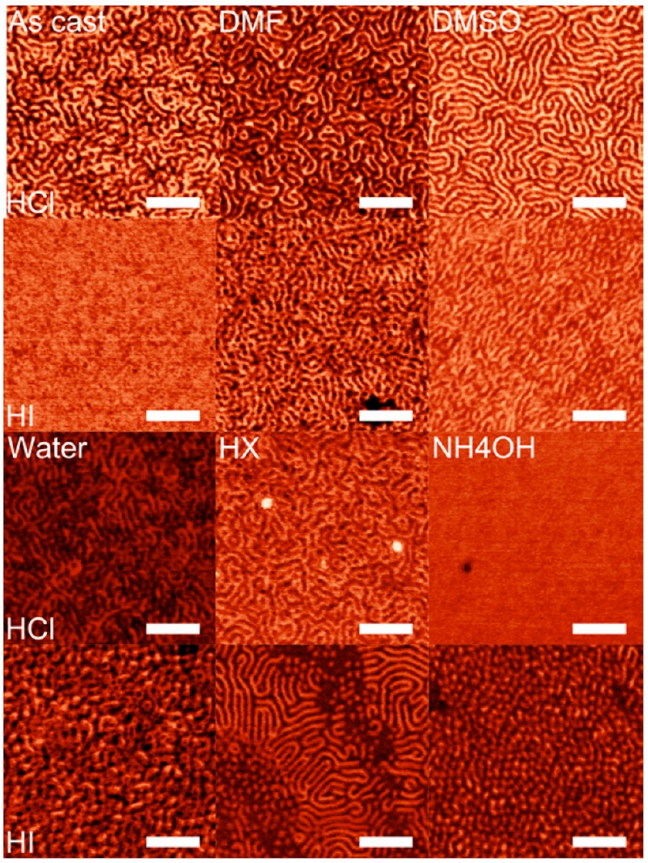

Figure 3. SFM phase images showing the effect of solvent annealing condition on polymer morphology. POEGMA50-P2VP30 diblocks with HCl or HI added to 55% stoichiometry with different solvent vapor anneals are displayed below. For the acid annealing case, each film was annealed in vapor of the same acid from which it was cast at 0.1 N concentration. The scale bars are 250 nm and the phase *z*-range is 25°.

Annealing in acidic or basic water vapor enables the degree of ionization of the polymer to be changed during solvent annealing, tuning interactions between the blocks during the annealing process. This means that it is a nonequilibrium processing step which can enhance the order dynamically as the composition of the material changes. However, transport through the vapor phase requires formation of uncharged HCl, HI, or NH_3 species, which are disfavored at equilibrium. Therefore, there is a severe mass transfer limit for the transport of these species through the vapor phase. As a result, the relatively low 0.1 N acid/base concentrations used in this work have a mild effect on P2VP charging during annealing (see Figure S4). At a higher acid concentration of 1 N, the acid transport into the film becomes more appreciable and can induce order in initially disordered acid-free films over a time scale of days (Figure S4).

Annealing in water results in weak order for both films; this is an enhancement for the HI-containing films which are disordered upon casting but almost no change for the HCl-containing films. Water provides mobility but also solubilizes the counterion and so it results in a reduced driving force for phase separation. Annealing in ammonium hydroxide has a similar effect to water on both films. The morphologies of the HI-containing film look very similar after both treatments and those of the HCl-containing films lose order in comparison to the organic solvent and as-cast cases. For the HCl-containing film ammonium hydroxide reduces the order as compared to annealing in water alone, suggesting that the ammonium is able to partially deprotonate vinylpyridine. The ammonium cation has a pK_a of 9.25, so at equilibrium there should be a transfer of protons from the pyridinium ions to the neutral ammonia molecules in the annealing vapor. This process is limited by kinetics and the protonation of some of the ammonia molecules by water.

In conclusion, miscible POEGMA-P2VP diblocks undergo disorder to order transitions when cast from acid-containing solutions due to protonation of the P2VP block. This ordering is caused by the formation of a pH-dependent ionomer, and the resultant structures can be tuned by intelligent combinations of counterion and solvent annealing. Acid-responsive self-assembly and pH-tunable aqueous processing are thus novel experimental techniques that can be used to tune and induce order in ion-containing copolymers.

■ ASSOCIATED CONTENT

Ⓢ Supporting Information

Gel permeation chromatography (GPC) and nuclear magnetic resonance (NMR) data from the block copolymers; SFM images that show that the time scale of acid incorporation during an acid anneal is longer than that used in this study. This material is available free of charge via the Internet at http://pubs.acs.org.

■ AUTHOR INFORMATION

Corresponding Author

*E-mail: bdolsen@mit.edu.

Notes

The authors declare no competing financial interest.

■ ACKNOWLEDGMENTS

Research supported as part of the Center for Excitonics, an Energy Frontier Research Center funded by the U.S. Department of Energy (DOE), Office of Science, Basic Energy Sciences (BES), under Award #DE-SC0001088 (thin film characterization) and by the National Science Foundation (NSF) under Award #CMMI-1246740 (polymer synthesis). NMR experiments were performed at the MIT Department of Chemistry Instrumentation Facility. Grazing incidence small-angle X-ray scattering was performed at the D1 line of the Cornell High Energy Synchrotron Source (CHESS), which is supported by the National Science Foundation and the National Institute of General Medical Sciences under NSF Award DMR-0936384

■ REFERENCES

(1) (a) Li, Q.; He, R.; Jensen, J. O.; Bjerrum, N. J. *Chem. Mater.* **2003**, *15* (26), 4896−4915. (b) Kreuer, K. *J. Membr. Sci.* **2001**, *185* (1), 29−39. (c) Hickner, M. A.; Ghassemi, H.; Kim, Y. S.; Einsla, B. R.; McGrath, J. E., Alternative polymer systems for proton exchange membranes (PEMs). *Chem. Rev.* **2004**, *104* (104587−4612); (d) Kerres, J. A. *J. Membr. Sci.* **2001**, *185* (1), 3−27.

(2) (a) MacFarlane, D. R.; Huang, J.; Forsyth, M. *Nature* **1999**, *402* (6763), 792−794. (b) Meyer, W. H. *Adv. Mater.* **1999**, *10* (6), 439−448. (c) Song, J.; Wang, Y.; Wan, C. *J. Power Sources* **1999**, *77* (2), 183−197.

(3) Mauritz, K. A.; Moore, R. B. *Chem. Rev.* **2004**, *104* (10), 4535−4586.

(4) (a) Croce, F.; Appetecchi, G.; Persi, L.; Scrosati, B. *Nature* **1998**, *394* (6692), 456−458. (b) Quartarone, E.; Mustarelli, P.; Magistris, A. *Solid State Ionics* **1998**, *110* (1−2), 1−14. (c) Marmorstein, D.; Yu, T.; Striebel, K.; McLarnon, F.; Hou, J.; Cairns, E. *J. Power Sources* **2000**, *89* (2), 219−226.
(5) (a) Elabd, Y. A.; Hickner, M. A. *Macromolecules* **2011**, *44* (1), 1−11. (b) Soo, P.; Huang, B.; Jang, Y.; Chiang, Y.; Sadoway, D.; Mayes, A. *J. Electrochem. Soc.* **1999**, *146* (1), 32−37. (c) Ruzette, A.; Soo, P.; Sadoway, D.; Mayes, A. *J. Electrochem. Soc.* **2001**, *148* (6), A537−A543.
(6) (a) Elabd, Y. A.; Walker, C. W.; Beyer, F. L. *J. Membr. Sci.* **2004**, *231* (1−2), 181−188. (b) Majewski, P. W.; Gopinadhan, M.; Jang, W.-S.; Lutkenhaus, J. L.; Osuji, C. O. *J. Am. Chem. Soc.* **2010**, *132* (49), 17516−17522.
(7) (a) Datye, V. K.; Taylor, P. L. *Macromolecules* **1984**, *17* (7), 1414−1415. (b) Duchesne, D.; Eisenberg, A. *Can. J. Chem.* **1990**, *68* (7), 1228−1232.
(8) (a) Ghosh, S. K.; De, P.; Khastgir, D.; De, S. *J. Appl. Polym. Sci.* **2000**, *78* (4), 743−750. (b) Antony, P.; Bandyopadhyay, S.; De, S. *J. Mater. Sci.* **1999**, *34* (11), 2553−2560.
(9) Weiss, R.; Izzo, E.; Mandelbaum, S. *Macromolecules* **2008**, *41* (9), 2978−2980.
(10) Shah, R. K.; Hunter, D.; Paul, D. *Polymer* **2005**, *46* (8), 2646−2662.
(11) Grady, B. P. *Polym. Eng. Sci.* **2008**, *48* (6), 1029−1051.
(12) (a) Weiss, R.; Sen, A.; Pottick, L.; Willis, C. *Polymer* **1991**, *32* (15), 2785−2792. (b) Lu, X.; Steckle, W.; Weiss, R. *Macromolecules* **1993**, *26* (22), 5876−5884. (c) Rubatat, L.; Shi, Z.; Diat, O.; Holdcroft, S.; Frisken, B. J. *Macromolecules* **2006**, *39* (21), 720−730.
(13) Park, M. J.; Balsara, N. B. *Macromolecules* **2008**, *41* (10), 3678−3687.
(14) Puterman, M.; Koenig, J.; Lando, J. *J. Macromol. Sci., Part B: Phys.* **1979**, *16* (1), 89−116.
(15) Gohy, J.-F.; Antoun, S.; Jerome, R. *Macromolecules* **2001**, *34* (21), 7435−7440.
(16) (a) Young, W.-S.; Epps, T. H. I. *Macromolecules* **2009**, *42* (7), 2672−2678. (b) Epps, T. H.; Bailey, T. S.; Waletzko, R.; Bates, F. S. *Macromolecules* **2003**, *36* (8), 2873−2881. (c) Epps, T. H.; Bailey, T. S.; Pham, H. D.; Bates, F. S. *Chem. Mater.* **2002**, *14* (4), 1706−1714. (d) Wang, J.-Y.; Chen, W.; Russell, T. P. *Macromolecules* **2008**, *41* (13), 4904−4907. (e) Wang, J.-Y.; Chen, W.; Roy, C.; Sievert, J. D.; Russell, T. P. *Macromolecules* **2008**, *41* (3), 963−969.
(17) Nakamura, I.; Balsara, N. P.; Wang, Z.-G. *Phys. Rev. Lett.* **2011**, *107* (19), 198301.
(18) (a) Wang, J.-Y.; Chen, W.; Sievert, J. D.; Russell, T. P. *Langmuir* **2008**, *24* (7), 3545−3550. (b) He, J.; Wang, J.-Y.; Xu, J.; Tangirala, R.; Shin, D.; Russell, T. P.; Li, X.; Wang, J. *Adv. Mater.* **2007**, *19* (24), 4370−4374. (c) Kim, S. H.; Misner, M. J.; Yang, L.; Gang, O.; Ocko, B. M.; Russell, T. P. *Macromolecules* **2006**, *39* (24), 8473−8479.
(19) Tantavichet, N.; Pritzker, M. D.; Burns, C. M. *J. Appl. Polym. Sci.* **2001**, *81* (6), 1493−1497.
(20) Brown, W.; Iverson, B.; Anslyn, E.; Foote, C. *Organic Chemistry*, 7the ed.; Wadsworth: Belmont, CA, 2014.
(21) Scudder, P. H. *Electron Flow in Organic Chemistry: A Decision-Based Guide to Organic Mechanisms*, 2nd ed.; John Wiley & Sons, Inc.: Hoboken, NJ, 2013.
(22) Sauer, B. B.; Dee, G. T. *Macromolecules* **2002**, *35* (18), 7024−7030.
(23) Bucholz, T. L. Design, synthesis, and characterization of functional block copolymers containing fluorinated or hydrophilic segments by ATRP. *Ph.D. Thesis*, University of Texas at Austin, Austin, TX, 2008.
(24) Lee, Y.-H.; Chang, C.-J.; Kao, C.-J.; Dai, C.-A. *Langmuir* **2010**, *26* (6), 4196−4206.
(25) Wang, Z.-G. *Phys. Rev. E* **2010**, *81* (2), 021501.
(26) (a) Huang, C.-I.; Lodge, T. P. *Macromolecules* **1998**, *31* (11), 3556−3565. (b) Hanley, K. J.; Lodge, T. P. *J. Polym. Sci., Part B: Polym. Phys.* **1998**, *37* (17), 3101−3113.